An electronic Duffing oscillator

Ghislain Raze

June 2024 - Rev 1.0

1 General schematics of the electronic Duffing oscillator

Figure 1 presents the (simplified) schematics of the electronic circuit used to implement a Duffing oscillator in [1], which is a slightly modified version of the circuit presented in [2, 3]. As shall be shown in Section 2, the relation between the input and output voltages, V_{in} and V_{out}, respectively, is a Duffing equation. An additional output V_1 is proportional to the time derivative of V_{out}. The circuit contains three operational amplifiers that make up two integrators and an inverting amplifier, three buffers, and two analog multipliers. Three potentiometers (p_1 - p_3) are used to tune the parameters of the circuit.

The practical realization in [1] also uses four additional switches and three additional buffers. The latter are needed to ensure low-impedance output and high-impedance input signals. As for the switches, three of them are used to enable the measurement of the division ratios of the potentiometers, and the fourth one can be used to obtain either a single- or double-well oscillator. The circuit requires an external power source with symmetric supplies. The input and output signals can be imposed/measured with BNC connectors.

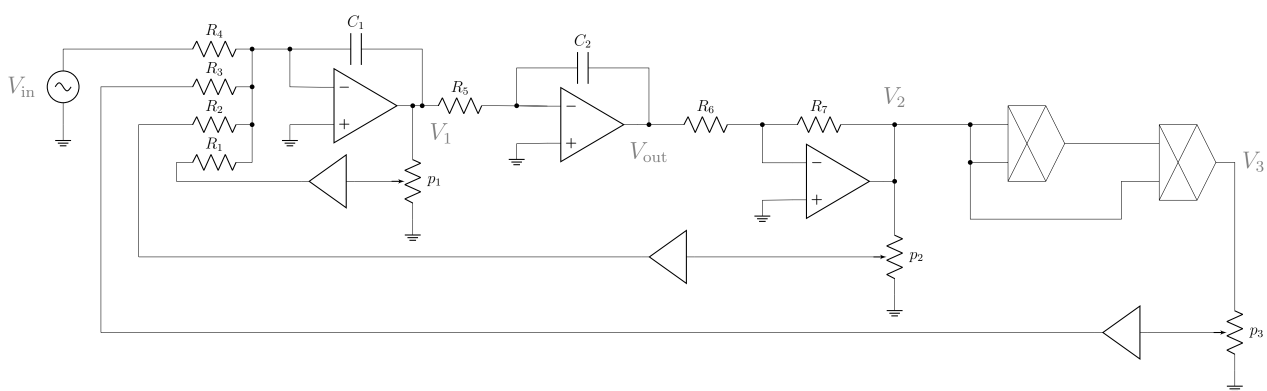

Figure 1: Schematics of the electronic Duffing oscillator.

2 Governing equations

The following section assumes ideal operational amplifier behavior, i.e., no current flows into the input pins, and the voltage of these input pins is identical (due to the feedback action of the amplifier) [4]. It is also assumed that the buffers are perfect. Their output voltage is thus, from left to right, $p_i V_i$ ($0 \leq p_i \leq 1$) for $i = 1, 2, 3$, where p_1, p_2 and p_3 are the division ratios of the potentiometers.

Since the inverting input of the leftmost operational amplifier is (virtually) grounded, the currents going into R_1 to R_4 all go into C_1, summing up to I_1. This realizes a summing integrator governed by

$$\dot{V}_1 = -\frac{1}{C_1} I_1 = -\frac{1}{C_1}\left(\frac{p_1 V_1}{R_1} + \frac{p_2 V_2}{R_2} + \frac{p_3 V_3}{R_3} + \frac{V_{\text{in}}}{R_4}\right). \tag{1}$$

The inverting input of the middle operational amplifier is also (virtually) grounded, and since the current going into R_5 also goes into C_2, this circuit implements an integrator governed by

$$\dot{V}_{\text{out}} = -\frac{V_1}{C_2 R_5}. \tag{2}$$

Finally, since the inverting input of the rightmost amplifier is (virtually) grounded and the current going through R_6 also goes into R_7, the circuit implements an inverting amplifier, i.e.,

$$V_2 = -\frac{R_7 V_{\text{out}}}{R_6} \tag{3}$$

The output of the first multiplier is $g_{\text{m}} V_2^2$, and that of the third is

$$V_3 = g_{\text{m}}^2 V_2^3, \tag{4}$$

where g_{m} is the gain of the electronic multiplier. Assembling Equations (1)-(4), one obtains a second-order differential equation for V_{out}:

$$C_1 C_2 R_4 R_5 \ddot{V}_{\text{out}} + p_1 \frac{C_2 R_4 R_5}{R_1} \dot{V}_{\text{out}} + p_2 \frac{R_4 R_7}{R_2 R_6} V_{\text{out}} + p_3 \frac{g_{\text{m}}^2 R_4 R_7^3}{R_3 R_6^3} V_{\text{out}}^3 = V_{\text{in}}, \tag{5}$$

which is a Duffing equation.

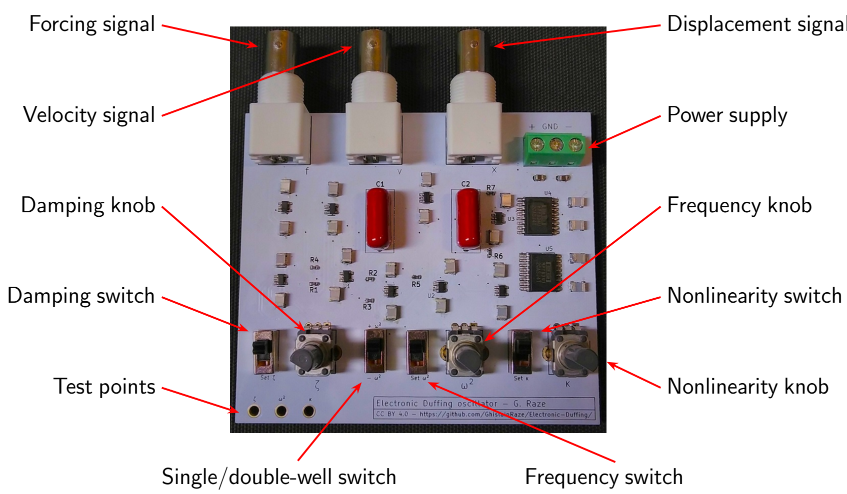

Figure 2: Picture of the electronic Duffing oscillator.

Figure 2 shows a photograph of the realization of the circuit in Figure 1 using Texas Instrument OPA210 operational amplifiers [5] and MPY634 multipliers [6].

3 Design choices

The electronic Duffing oscillator was designed to be interfaced with a MicroLabBox from dSPACE, hence had to be able to work with voltages in the $\pm 10\ V$ range. It was also desired to implement a weakly dissipative oscillator with very strong nonlinearity and relatively small resonance frequencies. These requirements guided the choice of the electrical parameters and integrated circuits, as briefly discussed in this section.

3.1 Electrical parameters

The rationale behind the choice of the electrical parameters of the circuit is now explained. Calculations were made based on the phase resonance backbone of the oscillator, which approximates the locus of maximum frequency response (for a weakly dissipative oscillator) [7].

Starting from Duffing's equation,

$$m\ddot{x}(t) + c\dot{x}(t) + kx(t) + k_3 x^3(t) = f\cos(\omega t); \tag{6}$$

it is assumed that the oscillator is at phase resonance and its response can be approximated by a one-harmonic Fourier series

$$x(t) = a\sin(\omega t). \tag{7}$$

Using the harmonic balance method, i.e., inserting this ansatz into Equation (6) and balancing fundamental sine and cosine coefficients, one obtains the two equations

$$\begin{cases} -m\omega^2 a + ka + \dfrac{3k_3}{4}a^3 = 0 \\ c\omega a = f \end{cases} \tag{8}$$

Inserting the second equation into the first one,

$$m\omega^2 - k - \frac{3k_3}{4}\frac{f^2}{c^2\omega^2} = 0, \tag{9}$$

from which the phase resonance backbone expression can be deduced as

$$\omega = \sqrt{\frac{k + \sqrt{k^2 + \dfrac{3mk_3 f^2}{c^2}}}{2m}}. \tag{10}$$

This frequency can also be normalized with the natural frequency of the underlying linear oscillator ($\omega_0^2 = k/m$)

$$\frac{\omega}{\omega_0} = \sqrt{\frac{1 + \sqrt{1 + \dfrac{3mk_3 f^2}{k^2c^2}}}{2}}, \tag{11}$$

and the amplitude of the phase resonance backbone can be found with the second relation in Equation (8)

$$a = \frac{f}{c\omega}. \tag{12}$$

Equation (6) has four parameters, namely m, c, k and k_3, that can be imposed to determine constraints that must be satisfied by the electrical parameters featured in Equation (5) (with $x \equiv V_{\mathrm{out}}$ and $f \equiv V_{\mathrm{in}}$). Alternatively, more meaningful parameters, such as the linear natural frequency $\omega_0 = \sqrt{|k|/m}$, the damping ratio $\zeta_0 = 2c/(m\omega_0)$, as well as the frequency ratio $\omega_{\max}/\omega_0$ and the forcing level f when the oscillator undergoes maximum-amplitude oscillations ($a = a_{\max}$) can be imposed.

Considerations should be given to saturation of the integrated circuits when the oscillator is in its extreme regimes. Since $V_{\mathrm{out}} \approx a$, the second operational amplifier should only saturate close to the most extreme regime ($a = a_{\max}$). To guarantee that the third operational amplifier (V_2) does not saturate before the second one, one can choose $R_6 = R_7$ (hence the amplitude of the voltage signals V_{out} and V_2 will be identical, as per Equation (3)). As for V_3, since $g_{\mathrm{m}} = 0.1$, the multipliers will saturate only if V_2 saturates. Finally, concerning V_1, Equations (2) and (7) show that

$$|V_1|_{\max} \approx C_2 R_5 \omega_{\max} a_{\max}, \tag{13}$$

which puts the constraint $C_2 R_5 \omega_{\max} \leq 1$ to avoid saturation of the first operational amplifier.

There can thus be seven constraints on the nine free parameters (seven resistances and two capacitances) depending on the user requirements. The electrical parameters may be selected depending on the commercially available electrical elements. Extreme values (low or high) could create undesirable loading effects and should be avoided.

3.2 Integrated circuits choice

OPA210 are precision operational amplifiers with very low offset voltage ($\leq 5\ \mu V$), which was the main motivation for their selection, together with their supply voltage range ($V_{\mathrm{s}} = \pm 18\ V$). In addition, they feature a large bandwidth for this application (GBW = 18 MHz) for a relatively low quiescent current [5]. For simplicity, buffers were realized with the same operational amplifiers in an input follower configuration.

The MPY634 analog multipliers were chosen for their availability, for their wide bandwidth (10 MHz) and for their adequate voltage range [6].

3.3 Other elements

Bipolar capacitors with high capacitances were needed to allow for relatively low resonance frequencies (in order to require reasonable resistances). Most dielectric materials with a high dielectric constant generally also feature high dissipation, which entails parasitic damping in the oscillator that can be complicated to model. Polypropylene (PP) film capacitors were thus selected for C_1 and C_2 due to their low dissipation, since their relatively large volume is not a problem in this application.

Lossy integrators can be used instead of the integrators implemented with the first and second operational amplifiers by placing a resistor with large resistance in parallel to C_1 and/or C_2. Since there was no saturation issue with the integrators, and since the offsets are quite small in the tested version of the circuit, this was not deemed necessary.

Following the application note, bypass capacitors of 0.1μF were used for all integrated circuits [5], and bulk capacitors of 10μF were used for the power supply.

3.4 Parameter values

The design considerations outlined herein led to the parameters gathered in Table 1. Note that the potentiometers allow for a flexible range of parameters c, k and k_3, but if the extreme values of these ranges are not satisfactory, other resistances and/or capacitances should be selected.

Parameter	Value
R_1 (kΩ)	100
R_2 (kΩ)	10
R_3 (kΩ)	1
R_4 (kΩ)	100
R_5 (kΩ)	1
R_6 (kΩ)	10
R_7 (kΩ)	10
C_1 (μF)	1
C_2 (μF)	1
g_{m} (V^{-1})	0.1

Table 1: Electrical parameters of the electronic Duffing oscillator.

4 Circuit implementation

4.1 Use of the circuit

The electrical Duffing oscillator can be used in an experimental setup. This section briefly describes how to use the printed circuit board (PCB) in [1]. The reader can refer to Figure 2 to identify the different elements on the PCB.

BNC connectors are used to drive the circuit via the forcing signal port (symbol `f` on the PCB for V_{in}) and to measure its output (symbols `x` and `v` on the PCB for V_{out} and for V_1, respectively). The circuit requires an external DC power source with symmetric supplies connected to the terminal block in the top right corner of the PCB. The supply voltage can range from $\pm 8\ V$ to $\pm 18\ V$ to comply with the maximum ratings of the integrated circuits [5, 6].

The parameters m, c, k and k_3 in Equation (6) can be computed by a simple comparison with Equation (5). The value of p_1, p_2 and p_3 can be adjusted by turning the knobs of the potentiometers. The switches `Set` ζ, `Set` ω^2 and `Set` κ on the PCB need to be up when the circuit is in operation, but can be down to make the determination of the value of these parameters easy when the circuit is not in operation. When they are down, they connect the potentiometers p_1, p_2 and p_3 (respectively) to the positive power supply. The output of the buffer connected to the potentiometer is also connected to a test point (vias) in the bottom left of the PCB (ζ, ω^2 and κ on the PCB, respectively). If the positive supply voltage is V_{s} and the switches are down, the voltage measured at these test points should be equal to $p_i V_{\mathrm{s}}$, allowing the user to deduce the value of p_i.

The last switch ($\pm\omega^2$ on the PCB) is used to implement a single- or double-well oscillator, when the switch is up or down, respectively. In the latter case, p_2 is connected to V_{out} instead of V_2 (cf. Figure 1).

4.2 Non-ideal behavior

Although the circuit does replicate the dynamics of a Duffing oscillator quite faithfully, this replication is not perfect due to several non-idealities. The ones suspected to be the most impactful are listed hereafter:

1. **Voltage offsets:** there exists voltage offsets at the input and output of the different integrated circuits, preventing a perfect symmetry in the oscillator.
2. **Imperfect integrators:** due to its finite open-loop gain, an operational amplifier used in an integrator will not perform an exact integration [5]. As also mentioned earlier, dissipation in the capacitors may also be the cause for an imperfect integrator behavior.
3. **Imperfect nonlinearity:** analog multipliers can also feature a small error (the output will not exactly be the product of the input voltages) [6].

5 Validation

Table 1 gathers the electrical parameters of the electronic oscillator. The potentiometers were adjusted to have a small dissipation ($p_1 = 0.1311$), relatively small resonance frequency ($p_2 = 0.1923$) and maximized nonlinearity ($p_3 = 0.9887$). From these values and those in Table 1, using Equation (5), it was possible to deduce the theoretical characteristics of the oscillator given in Table 2. They were compared to an identification with the nonlinear frequency subspace identification (FNSI) method [8] using data from a swept-up sine test between 50 and 200 rad/s with a forcing amplitude of 0.03 V.

Table 2: Theoretical and identified parameters of the electronic Duffing oscillator.

Parameter	**Theoretical value**	**Identified value**
m (s^2)	10^{-4}	1.0461×10^{-4}
c (s)	1.3×10^{-4}	1.4231×10^{-4}
k (-)	1.923	1.8099
k_3 (V^{-2})	0.9887	1.0077

Small differences can be observed between theoretical and experimental values. Part of it can be attributed to the uncertainty on the capacitances ($\pm5\%$). There could also be non-idealities in the circuit that may come from non-ideal operational amplifiers and multipliers characteristics.

References

[1] G. Raze, “An electronic Duffing oscillator,” 2024. [Online]. Available: https://github.com/GhislainRaze/Electronic-Duffing

[2] B. K. Jones and G. Trefan, “The Duffing oscillator: A precise electronic analog chaos demonstrator for the undergraduate laboratory,” *Am. J. Phys.*, vol. 69, no. 4, pp. 464–469, apr 2001. [Online]. Available: https://pubs.aip.org/aapt/ajp/article/69/4/464-469/1055595

[3] K. Srinivasan, K. Thamilmaran, and A. Venkatesan, “Effect of nonsinusoidal periodic forces in Duffing oscillator: Numerical and analog simulation studies,” *Chaos, Solitons & Fractals*, vol. 40, no. 1, pp. 319–330, apr 2009. [Online]. Available: https://linkinghub.elsevier.com/retrieve/pii/S0960077907005796

[4] P. Horowitz and W. Hill, *The Art of Electronics*, 3rd ed. Cambridge University Press, 2015.

[5] *OPAx210 2.2-nV/$\sqrt{Hz}$ Precision, Low-Power, 36-V Operational Amplifiers*, Texas Instruments, 08 2021. [Online]. Available: https://www.ti.com/lit/ds/symlink/opa210.pdf

[6] *Wide Bandwidth PRECISION ANALOG MULTIPLIER*, Texas Instruments, 2004. [Online]. Available: https://www.ti.com/lit/ds/symlink/mpy634.pdf

[7] M. Cenedese and G. Haller, “How do conservative backbone curves perturb into forced responses? A Melnikov function analysis,” *Proceedings of the Royal Society A: Mathematical, Physical and Engineering Sciences*, vol. 476, no. 2234, p. 20190494, feb 2020. [Online]. Available: https://royalsocietypublishing.org/doi/10.1098/rspa.2019.0494

[8] J. Noël and G. Kerschen, “Frequency-domain subspace identification for nonlinear mechanical systems,” *Mechanical Systems and Signal Processing*, vol. 40, no. 2, pp. 701–717, nov 2013. [Online]. Available: https://linkinghub.elsevier.com/retrieve/pii/S088832701300318X